life

MDPI

Article

RETRACTED: Secukinumab and Black Garlic Downregulate OPG/RANK/RANKL Axis and Devitalize Myocardial Interstitial Fibrosis Induced by Sunitinib in Experimental Rats

Hoda E. Mohamad [1,*], Mervat E. Asker [1], Mohamed A. Shaheen [2], Nourhan M. Baraka [1], Omer I. Fantoukh [3], Abdulaziz Alqahtani [3], Alaa E. Salama [4] and Yasmin K. Mahmoud [1]

[1] Department of Biochemistry, Faculty of Pharmacy, Zagazig University, Zagazig 44519, Egypt
[2] Department of Histology & Cell Biology, Faculty of Medicine, Zagazig University, Zagazig 44519, Egypt
[3] Department of Pharmacognosy, College of Pharmacy, King Saud University, Riyadh 11451, Saudi Arabia
[4] Department of Cardiology, Faculty of Medicine, Zagazig University, Zagazig 44519, Egypt
* Correspondence: hmohammed@zu.edu.eg; Tel.: +20-10-2799-4483

Abstract: Sunitinib has been associated with several cardiotoxic effects such as cardiac fibrosis. The present study was designed to explore the role of interleukin (IL)-17 in sunitinib-induced myocardial fibrosis (MF) in rats and whether its neutralization and/or administration of black garlic (BG), a form of fermented raw garlic (*Allium sativum* L.), could extenuate this adverse effect. Male Wistar albino rats received sunitinib (25 mg/kg three times a week, orally) and were co-treated with secukinumab (3 mg/kg, subcutaneously, three times total) and/or BG (300 mg/kg/day, orally) for four weeks. Administration of sunitinib induced significant increase in cardiac index, cardiac inflammatory markers, and cardiac dysfunction that were ameliorated by both secukinumab and BG, and to a preferable extent, with the combined treatment. Histological examination revealed disruption in the myocardial architecture and interstitial fibrosis in cardiac sections of the sunitinib group, which were reversed by both secukinumab and BG treatments. Both drugs and their co-administration restored normal cardiac functions, downregulated cardiac inflammatory cytokines, mainly IL-17 and NF-κB, along with increasing the MMP1/TIMP1 ratio. Additionally, they attenuated sunitinib-induced upregulation of the OPG/RANK/RANKL axis. These findings highlight another new mechanism through which sunitinib can induce interstitial MF. The current results propose that neutralizing IL-17 by secukinumab and/or supplementation with BG can be a promising therapeutic approach for ameliorating sunitinib-induced MF.

Keywords: sunitinib; secukinumab; black garlic; interstitial myocardial fibrosis; IL-17; OPG/RANK/RANKL

check for updates

Citation: Mohamad, H.E.; Asker, M.E.; Shaheen, M.A.; Baraka, N.M.; Fantoukh, O.I.; Alqahtani, A.; Salama, A.E.; Mahmoud, Y.K. RETRACTED: Secukinumab and Black Garlic Downregulate OPG/RANK/RANKL Axis and Devitalize Myocardial Interstitial Fibrosis Induced by Sunitinib in Experimental Rats. *Life* **2023**, *13*, 308. https://doi.org/10.3390/life13020308

Academic Editor: Stefania Lamponi

Received: 23 December 2022
Revised: 18 January 2023
Accepted: 20 January 2023
Published: 22 January 2023
Retracted: 14 July 2026

Copyright: © 2023 by the authors. Licensee MDPI, Basel, Switzerland. This article is an open access article distributed under the terms and conditions of the Creative Commons Attribution (CC BY) license (https://creativecommons.org/licenses/by/4.0/).

1. Introduction

Targeted chemotherapy by tyrosine kinase inhibitors (TKIs) is a highly selective advancement that has enhanced antitumor activity with reducing toxicities in comparison to conventional chemotherapies [1]. Nevertheless, the cardiotoxicity of TKIs has emerged beside their anti-cancer potencies [2]. Sunitinib (SUN) is an orally active TKI approved for treating various types of carcinomas [3]. Although SUN has showed great effectiveness, its clinical efficacy is limited due to its cardiac toxicities, such as hypertension, myocardial infarction (MI), and fibrosis [4]. However, the underlying mechanisms involved in these cardiotoxic effects are still unclear.

Myocardial fibrosis (MF) is one of the cardiac events that results from using SUN [5]. It results from the disruption of equilibrium between synthesis and degradation of collagen [6]. This equilibrium is regulated by matrix metalloproteinases (MMPs) and tissue inhibitors of metalloproteinase (TIMP), in which their expressions were found to be elevated during MF [7].

Inflammation also plays an important role in MF, and both occur within the same damaged region following cardiomyopathy and MI [8,9]. In the early stages of inflammation,

This paper has been retracted. A retraction notice was published on 14 July 2026 in *Life* **2026**, *16*, 1165. https://doi.org/10.3390/life16071165

RETRACTED

cytokines such as interleukin- 17 (IL-17) induce fibrotic cell formation to repair the injured regions and this continuous release of cytokines stimulates MF [10]. This renders IL-17 to be one of the most important contributors to MF and its inhibition may exhibit benefits in preventing these complications.

Osteoprotegerin (OPG), a member of the tumor necrosis factor (TNF) receptor family, competitively inhibits the interaction between receptor activator of nuclear factor-κB (RANK) and its ligand (RANKL) [11]. It is known that the OPG/RANK/RANKL system plays a central role in bone homeostasis [12]. However, previous studies have found that this system is also strongly associated with ventricular remodeling after MI and cardiac fibrosis [13–15].

Secukinumab (SEC) is a human monoclonal antibody that selectively targets and blocks IL-17A interaction with the IL-17 receptor. It demonstrates long-lasting efficacy in patients with psoriasis and ankylosing spondylitis [16,17]. In addition, a recent study demonstrated a promising antifibrotic effect of SEC against dermal fibrosis [18].

Black garlic (BG) is one of the most studied garlic products for its magnificent beneficial impact on human health [19]. It is prepared by subjecting raw garlic (*Allium sativum* L.) to high temperature and humidity via the Millard reaction. This aging process not only modifies the offensive odor of fresh garlic but also improves BG bioactivity. BG health benefits are related to the presence of various bioactive compounds such as amino acids, including L-methionine, L-arginine and L-cysteine, minerals, reducing sugars, flavonoids, 5-hydroxymethyl furfural, organosulfur compounds, S-allyl cysteine (SAC) and melanoidins. SAC is regarded as the main active ingredient of BG [20]. Multiple studies demonstrated that SAC revealed a cardiovascular protective action against myocardial injury and infarction due to its antioxidant capacity that is associated with the reduction of products of lipid peroxidation. Besides its antioxidative effect, SAC also possesses hepato-protective and anti-cancer activities [21–24].

Accordingly, the current study has been initiated to investigate whether IL-17 alters the mediators engaged in MF and if so, whether this alteration would be viewed as a mechanism during development of SUN-induced cardiotoxicity, mainly myocardial interstitial fibrosis. Another important goal is to further explore one of the molecular mechanisms whereby IL-17 neutralization and BG supplementation could mitigate SUN-induced MF.

2. Materials and Methods

2.1. Drugs

Sunitinib (Sutent® 50 mg) was purchased from Pfizer, USA. Secukinumab (Cosentyx® 150 mg/mL prefilled pen) was supplied from Novartis, USA. Black garlic (400 mg fermented garlic bulb, 0.6 mg SAC) was provided from Dr Mercola, USA.

2.2. Animals

Eight-week-old male Wistar albino rats weighing 180 ± 20 g were purchased from the Experimental Animal Center, Faculty of Veterinary Medicine, Zagazig University, Zagazig, Egypt and housed in a temperature- and humidity-controlled environment under a 12 h light/dark cycles. The rats had access to a standard diet and water. Animal care and all experimental procedures were executed according to protocols approved by the institutional committee of laboratory animal care and use of Zagazig University (Protocol # ZU-IACUC/3/F/183/2021) and in accordance with NIH guidelines for animal research.

2.3. Experimental Protocol

Fifty rats were divided into two main experimental groups: the normal control group (NC, n = 10) received water orally and the sunitinib group (n = 40) received an oral dose of sunitinib (25 mg/kg three times a week) for 4 weeks and sub-divided into four subgroups (n = 10/group) as following: SUN group: rats received only the oral dose of sunitinib and did not receive any other treatments; SEC group: rats received the oral dose of sunitinib

RETRACTED

and treated concurrently with secukinumab (3 mg/kg, subcutaneously) at weeks 0, 2, and 4; BG group: rats received the oral dose of sunitinib and treated concurrently with black garlic (300 mg/kg/day, orally [25]); SEC + BG group: rats received the oral dose of sunitinib and treated concurrently with secukinumab and black garlic by the same doses previously mentioned. Secukinumab dose concentration was adapted according to previous studies [16,26]. The selected dose of SUN was chosen after our experimental trials to induce cardiotoxicity in rats and was adapted from Imam et al. [27] (Supplementary Figure S1 and Table S1). Docking study was performed to ensure the efficacy of using secukinumab (human monoclonal antibody) against rat IL-17A in this study (Supplementary Figure S2 and Table S2).

2.4. Echocardiography

At the end of the experiment, rats were weighed and anesthetized using ketamine/xylazine (50:1) [28]. Echocardiography was conducted to measure: left ventricular ejection fraction% (LVEF%) and fractional shortening % (FS%). Values of at least three measurements were obtained for each rat [29].

2.5. Blood Pressures and Heart Rate Measurements

Systolic, diastolic, and mean blood pressures (SBP, DBP, and MBP), as well as heart rate (HR), were measured at the end of the study according to Parasuraman et al. as described previously [30]. Briefly, anesthetized rats were subjected to tracheostomy and the carotid artery was recognized and cannulated with a heparinized normal saline-filled cannula. Three measurements were obtained for each rat and an average value was calculated.

2.6. Blood and Tissue Samples Collection

At the end of the experimental study, rats were fasted overnight, weighed, then killed by decapitation under pentobarbital sodium anesthesia (40 mg/kg, I.P) [15,31]. Blood samples were collected via Retro-orbital plexus and centrifuged (3000× *g*) at 4 °C for 10 min. to separate the serum. Aliquots of serum were frozen at −20 °C for further biochemical assays. Intact hearts were rapidly dissected, rinsed with ice-cold 0.9% saline solution, dried, and weighed to calculate the cardiac index (CI) for each rat, which represents the ratio of the heart weight to the body weight (g/100 g). Some parts of heart tissues were snap-frozen in liquid nitrogen and then stored at −20 °C for subsequent analysis. The other parts were fixed in 10% buffered formalin for 24 h for histological analysis.

2.7. Biochemical Measurements

Serum C-reactive protein (CRP) levels were assessed by enzyme-linked immunesorbent assay (ELISA) using a commercially available rat ELISA kit (BD Biosciences, San Jose, CA, USA, catalog # 557825) according to the supplier's guidelines. Serum levels of creatine kinase-MB (CK-MB) were measured using a commercially available kit (Spinreact Co., Girona, Spain, catalog # BEIS04-1) following the manufacturer's instructions.

2.8. Enzyme-Linked Immunosorbent Assay (ELISA)

Heart tissue homogenate (10%) was prepared in 0.05 M phosphate buffer (pH = 7) using a polytron homogenizer at 4 °C. The homogenate was centrifuged at 10,000 rpm for 20 min to remove the cell debris. The supernatant was used for determination of cardiac nuclear factor kappa B (NF-κB) (Cusabio, Houston, TX, USA, catalog # CSB-E13148r), cardiac inflammatory cytokines; IL-1β, IL-6, and IL-17 (Cusabio, Houston, TX, USA, catalog #CSB-E08055r, CSB-E04640r and CSB-E07451r, respectively) and cardiac TNF-α (SunLong Biotech Co, Hangzhou, Zhejiang, China, catalog # SL0722Ra) using rat ELISA kits following the manufacturer's instructions.

RETRACTED

2.9. Real-Time Polymerase Chain Reaction (RT-PCR)

Total RNA was extracted from cardiac tissue homogenate with the High Pure RNA Isolation Kit (Roche Diagnostics GmbH, Mannheim, Germany, catalog # 11 828 665 001) and reverse-transcribed using Quanti Tects Reverse Transcription Kit (Qiagen, Germantown, Maryland, USA) according to the manufacturer's instructions. The quantity and quality were assessed by Beckman dual spectrophotometer (USA). cDNA was then amplified using Maximas SYBR Green/Fluorescein qPCR Master Mix and following the primer sequences in Table 1. Thermal cycling conditions were designed according to Lanoix et al. [32] as follows: denaturation for 8 min at 94 °C, followed by 40 cycles of 30 s denaturing at 94 °C, 45 s annealing at 56 °C, and 50 s extension at 72 °C with a final extension of 7 min at 72 °C. The relative mRNA genes expression of the MMP1 andTIMP1 were analyzed and normalized against the internal control glyceraldehyde-3-phosphate dehydrogenase (GAPDH), using the cycle threshold ($2^{-\Delta\Delta ct}$) method.

Table 1. Primers sequences.

	Forward Sequence	Reverse Sequence
MMP1	5′-ATGCTGAAACCCTGAAGGTG-3′	5′-GAGCATCCCCTCCAATACCT-3′
TIMP1	5′-CGCAGCGAGGAGGTTTCTCAT-3′	5′-GGCAGTGATGTGCAAATTTCC-3′
GAPDH	5′- TGAAGGTCGGAGTCAACGGATTTGGT-3′	5′ -CATGTGGGCCATGAGGTCCACCAC-3′

2.10. Western Blot Analysis

Heart tissues were lysed with a TriFast (Peqlab, VWR Company, USA). Centrifugation at 12,000× *g* at 4 °C for 10 min was performed to separate the supernatant. Then, total protein concentrations were determined using the Bradford protein assay method [33]. Proteins (20 µg) were fractionated by 10% gel electrophoresis and transferred to polyvinylidene fluoride membranes and then blocked in Tris buffered saline, containing 5% skimmed milk. The membrane was incubated overnight at 4 °C with the specific primary antibodies purchased from (Abcam, USA), including antibody solution containing Anti-OPG antibody (1 µg/mL, catalog # ab73400), Anti-RANK antibody (catalog # ab200369), and Anti-RANKL antibody (0.5–5 µg/mL, catalog # ab239607). After incubation with the correct secondary antibodies, immunoreactive proteins were visualized using an ECL chemiluminescence detection kit (Bio-Rad, Hercules, CA, USA) with subsequent autoradiography. Stripped membranes were reprobed with primary antibody for β-actin (1 µg/mL, Sigma, St. Louis, MO, USA) to ensure equal protein loading. A gel documentation system (Geldoc-it, UVP, England) was applied for data analysis using total lab. analysis software, (Ver.1.0.1) and the amounts of the proteins were normalized to their corresponding β-actin control.

2.11. Histological Analysis

After fixation in buffered neutral formalin, the heart tissues were dehydrated in gradual ascending concentrations of ethanol, cleared in xylene, and embedded in paraffin. Thick sections (5 µm) were cut using a microtome (Leica RM 2155, UK) and stained with Hematoxylin and Eosin (H&E) and Van Gieson stain according to the standard procedures and evaluated under light microscopy (Olympus BX50, Olympus, Tokyo, Japan). Ten randomly selected microscopic fields in Van Gieson-stained sections were analyzed and averaged for each rat to assess the degree of interstitial fibrosis. Myocardial fibrosis was quantified as the area percentage of fibrotic area of collagen/µm2 using Image-Pro Plus software, version 6.0 (Media Cybernetics), as previously reported [34].

2.12. Statistics

All data were expressed as mean ± SD. Statistical analysis was performed using GraphPad Prism 5 (GraphPad Software, Inc., San Diego, CA, USA). One-way analysis of variance (ANOVA) followed by Tukey's post hoc test were used to determine the level of significance. A value of $p < 0.05$ was considered statistically significant.

RETRACTED

3. Results

3.1. Body and Heart Weights and Cardiac Index (CI)

As shown in Table 2, there was an obvious decrease in body weight (by 32.2%) in addition to an elevation in heart weight (by 60.2%) and CI (by 136.7%) in the SUN group as compared to the normal control ($p < 0.001$), which were alleviated by secukinumab or black garlic treatments in comparison to the SUN group. Interestingly, concomitant administration of secukinumab and black garlic exhibited better effects than the individual therapies.

Table 2. Effect of treatment with secukinumab and/or black garlic supplement on body and heart weights, CI, serum CRP, and CK-MB levels of SUN-administered rats.

	NC	SUN	SEC	BG	SEC + BG
Body weight (g)	324.8 ± 7.55	220.3 ±6.12 [a]	270 ± 6.87 [b]	250.7 ± 7 [b]	300.5 ± 6.38 [b,#,$]
Heart weight (g)	0.98 ± 0.07	1.57 ± 0.07 [a]	1.29 ± 0.04 [b]	1.42 ± 0.07 [b]	1.13± 0.06 [b,#,$]
CI (g/100 g)	0.3 ± 0.01	0.71 ± 0.01 [a]	0.48 ± 0.005 [b]	0.57 ± 0.01 [b]	0.38± 0.01 [b,#,$]
CRP (ng/mL)	15.1 ± 3.61	298.9 ± 57.17 [a]	97.6 ± 9.86 [b]	168.1 ± 17.1 [b]	36.88 ± 5.23 [b,#,$]
CK-MB (U/L)	439.7 ± 44.37	959.9 ± 26.94 [a]	686 ± 18.95 [b]	778.4 ± 15.34 [b]	546.8± 25.73 [b,#,$]

The data are expressed as mean ± SD, (n = 6/group), SD: Standard deviation; n: Sample size. CI: cardiac index; CRP: C-reactive protein; CK-MB: creatine kinase–MB; NC: normal control; SUN: sunitinib; SEC: secukinumab; BG: black garlic. [a] $p < 0.001$ vs. NC, [b] $p < 0.01$ vs. SUN, [#] $p < 0.05$ vs. BG, [$] $p < 0.01$ vs. SEC.

3.2. Serum Inflammatory and Cardiotoxic Enzyme Markers

To confirm that the SUN treatment protocol used in this study is associated with cardiotoxicity, the effect of SUN on serum inflammatory protein; CRP and cardiotoxicity enzymatic index; CK-MB, were studied in normal rats as well as in SUN, SEC, and BG treated rats (Table 2). A readable rise in serum CRP (1879%) and CK-MB (118%) was detected in rats treated with SUN compared to the normal ones ($p < 0.001$). However, such effect was significantly mitigated to a great extent by both the individual and the combined therapies in comparison to the SUN group. The best results were shown with the combined medication.

3.3. Blood Pressure and Left Ventricular Function

As depicted in Figure 1A–D, SUN-treated rats showed significantly raised SBP, DBP, MBP, as well as HR by 1.5, 1.8, 1.6, and 1.4-folds, respectively, compared to the control group ($p < 0.001$). Treatment with SEC or BG notably minimized the above-mentioned parameters as compared to the SUN group ($p < 0.05$). On the other hand, co-administration of SEC and BG showed better findings compared to the single treatments.

Moreover, our data revealed a reduction in both LVEF% and FS% in the SUN-induced cardiotoxicity group by 0.36 and 0.23-folds, respectively, compared to the healthy group ($p < 0.001$). All medications were able to markedly improve left ventricular function as indicated by the elevated LVEF % (by 1.76, 1.34, and 2.48-fold, respectively) and FS% (by 2.38, 1.56, and 3.46-fold, respectively) compared to the SUN group ($p < 0.01$), however, the greatest improvement was seen in the SEC+ BG group ($p < 0.001$) (Figure 1E–G).

RETRACTED

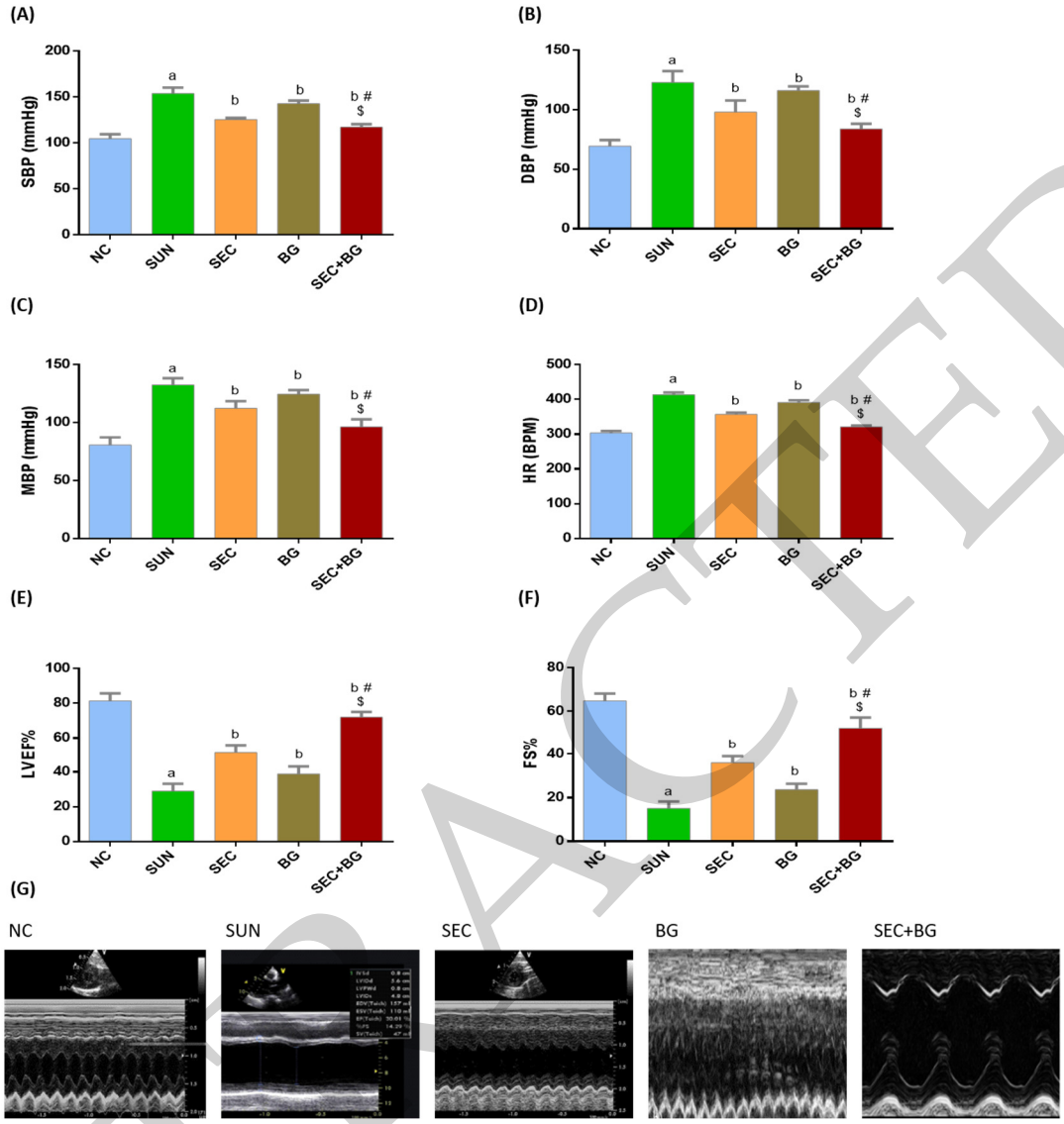


Figure 1. Effect of treatment with secukinumab and/or black garlic supplement on cardiac hemodynamic parameters and left ventricular function of SUN-administered rats. (**A**) SBP: systolic blood pressure. (**B**) DBP: diastolic blood pressure. (**C**) MBP: mean blood pressure. (**D**) HR: heart rate. (**E**) LVEF%: left ventricular ejection fraction. (**F**) FS%: fractional shortening. (**G**) Representative images of M-mode tracings through the left ventricles of the rats. Bars and error bars represent mean ±SD. (n = 6/group). NC: normal control; SUN: sunitinib; SEC: secukinumab; BG: black garlic. [a] $p < 0.001$ vs. NC, [b] $p < 0.05$ vs. SUN, [#] $p < 0.01$ vs. BG, [$] $p < 0.01$ vs. SEC.

3.4. Cardiac Cytokines and NF-κB

Regarding our results, the cardiac levels of IL-1β, IL-6, IL-17, TNF-α, and NF-κB were considerably upregulated in the SUN group in comparison with the NC group ($p < 0.001$). The suppressive effect of secukinumab alone on the aforementioned markers was significantly greater than that of black garlic alone. Co-administration of secukinumab and black garlic induced a marked down-regulation in the studied cytokines and NF-κB more than either monotherapy (Figure 2A–E).

RETRACTED

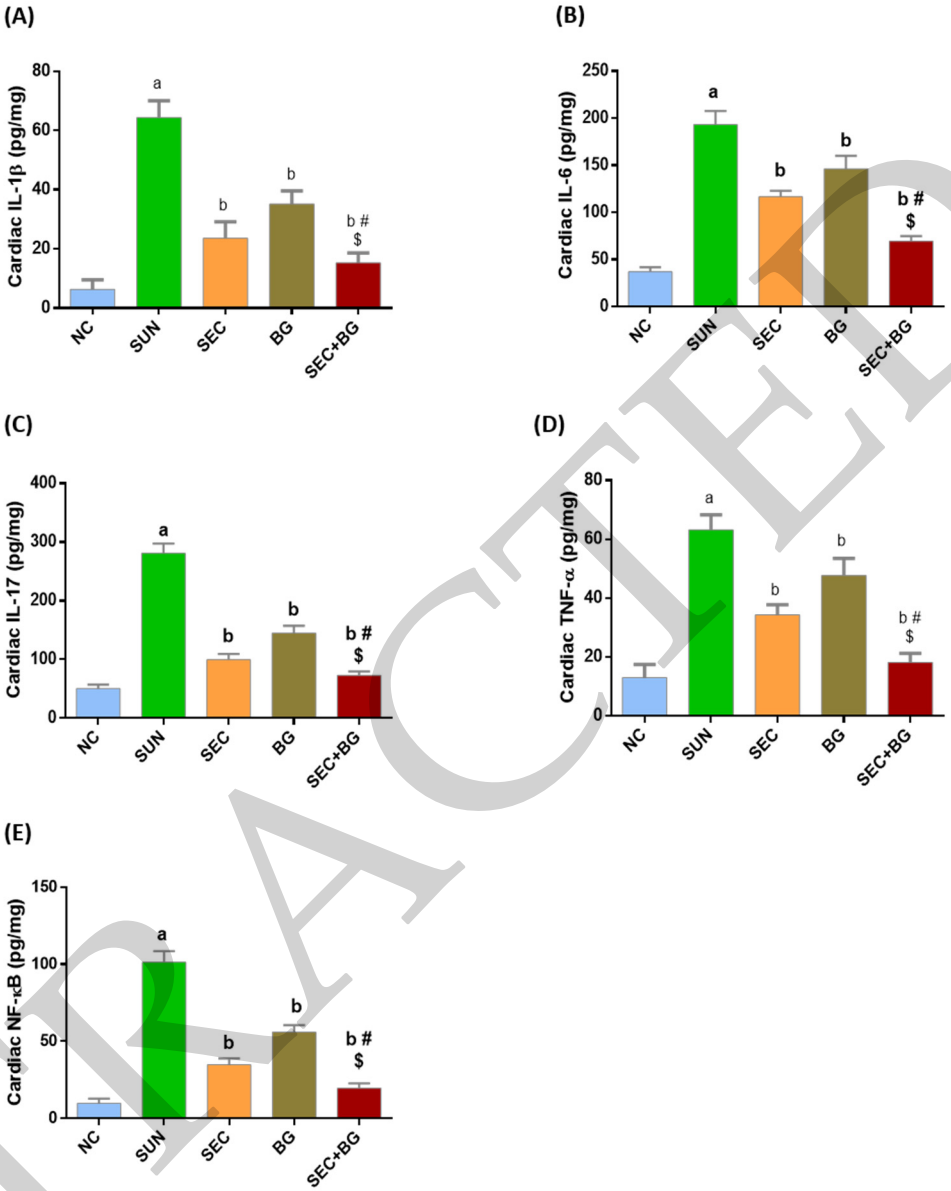


Figure 2. Effect of treatment with secukinumab and/or black garlic supplement on cardiac inflammatory markers and cytokines of SUN-administered rats. (**A**) IL-1β: interleukin-1β. (**B**) IL-6. (**C**) IL-17. (**D**) TNF-α: tumor necrosis factor-α. (**E**) NF-κB: nuclear factor kappa B. NC: normal control; SUN: sunitinib; SEC: secukinumab; BG: black garlic. Bars and error bars represent mean ± SD. (n = 6/group). [a] $p < 0.001$ vs. NC, [b] $p < 0.001$ vs. SUN, [#] $p < 0.01$ vs. BG, [$] $p < 0.001$ vs. SEC.

3.5. Cardiac Protein Expression of the OPG/RANK/RANKL Axis

As represented in Figure 3, the hearts of SUN-treated rats had markedly elevated protein expression of OPG, RANK, and RANKL, by 262%, 262%, and 370%, respectively, as compared to the normal group ($p < 0.001$). Nevertheless, OPG, RANK, and RANKL protein levels were diminished in the anti-IL-17, secukinumab, and black garlic groups. Importantly, combining secukinumab with black garlic showed a better attenuation in the OPG/RANK/RANKL axis.

RETRACTED

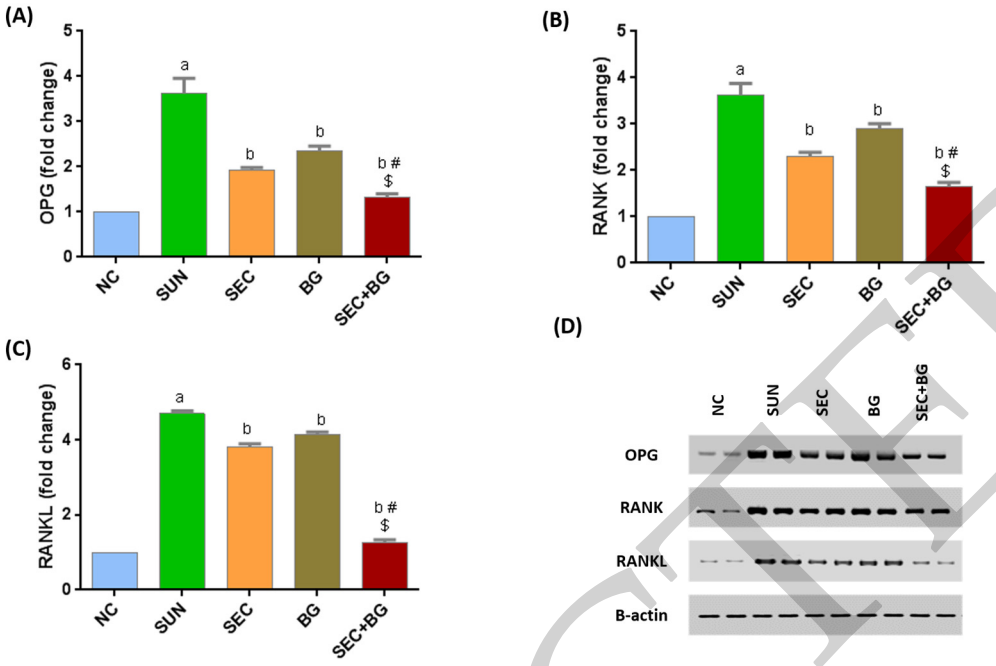


Figure 3. Effect of treatment with secukinumab and/or black garlic supplement on OPG/RANK/RANKL axis of SUN-administered rats. Quantitative analysis of: (**A**) Osteoprotegerin (OPG) expression, (**B**) receptor activator of nuclear factor-κB (RANK) expression, (**C**) RANK ligand (RANKL) expression; relative to β-actin, and (**D**) representative Western blot images. Bars and error bars represent mean ± SD. (n = 6/group). NC: normal control; SUN: sunitinib; SEC: secukinumab; BG: black garlic. [a] $p < 0.001$ vs. NC, [b] $p < 0.001$ vs. SUN, [#] $p < 0.001$ vs. BG, [$] $p < 0.001$ vs. SEC.

3.6. Cardiac MMP1 and TIMP1 Gene Expression and Extracellular Matrix Turnover Marker

As shown in Table 3, rats treated with SUN exhibited a 2.7 and 3.7-fold raise in MMP1 and TIMP1 mRNA expression levels, respectively, compared to the normal control group ($p < 0.001$). Consequently, the extracellular matrix turnover marker, MMP1/TIMP1 ratio was substantially decreased by 0.75-fold ($p < 0.001$). The MMP1/TIMP1 ratio was notably augmented upon administration of secukinumab (by 1.28-fold) or black garlic (by 1.16 fold) relative to the SUN group. Secukinumab and black garlic concurrent therapy showed the most prominent enhancement (by 1.5-fold vs. SUN group) in the MMP1/TIMP1 balance compared to the individual treatments.

Table 3. Effect of treatment with secukinumab and/or black garlic supplement on MMP1 and TIMP1 genes expression and MMP1/TIMP1 ratio of SUN-administered rats.

	NC	SUN	SEC	BG	SEC + BG
MMP1	0.94 ± 0.13	2.55 ± 0.13 [a]	1.79 ± 0.08 [b]	2.21 ± 0.08 [b]	1.29 ± 0.08 [b,#,$]
TIMP1	0.86 ± 0.10	3.14 ± 0.23 [a]	1.70 ± 0.09 [b]	2.33 ± 0.14 [b]	1.05 ± 0.09 [b,#,$]
MMP1/TIMP1	1.10 ± 0.03	0.82 ± 0.02 [a]	1.05± 0.01 [b]	0.95 ± 0.02 [b]	1.23± 0.02 [b,#,$]

The data are expressed as mean ± SD, (n = 6/group); SD: Standard deviation; n: Sample size. MMP1: matrix metalloproteinase 1; TIMP1: tissue inhibitor of metalloproteinase 1; NC: normal control; SUN: sunitinib; SEC: secukinumab; BG: black garlic. [a] $p < 0.001$ vs. NC, [b] $p < 0.05$ vs. SUN, [#] $p < 0.01$ vs. BG, [$] $p < 0.001$ vs. SEC.

3.7. Histological Findings

3.7.1. H&E Stain

Histopathological analysis of H & E-stained paraffin sections of the left ventricular myocardium of the control group showed striated myocardial fibers, which were arranged in transverse and longitudinal directions with their characteristic obvious intercalated discs.

RETRACTED

The cardiac muscle fibers appeared acidophilic with central bright vesicular nuclei. No inflammatory cellular infiltrations or vascular congestion were noticed. They were separated by scanty connective tissue containing fibroblasts with their flat nuclei (Figure 4A).

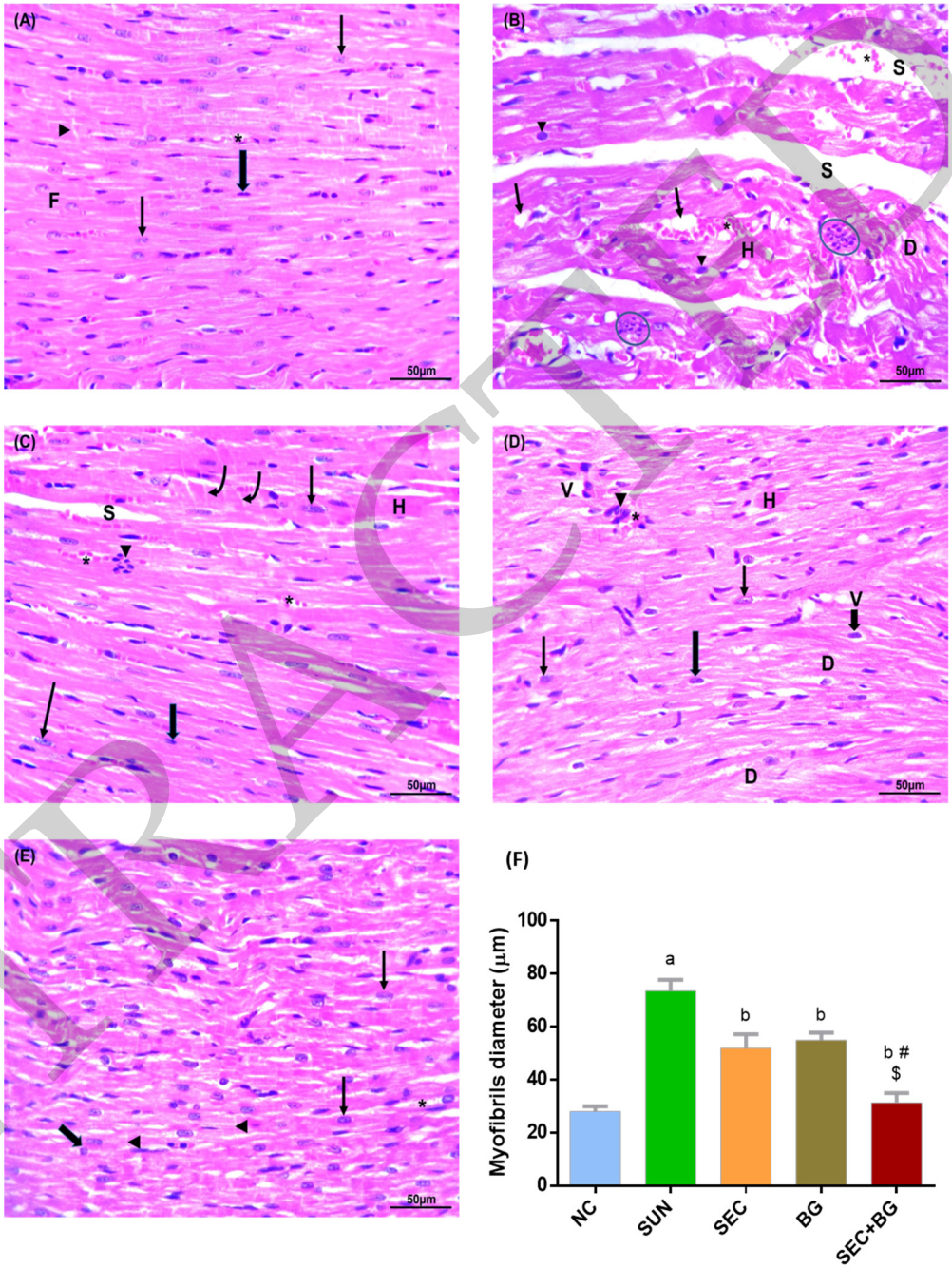


Figure 4. Representative photomicrographs of H&E-stained cardiac sections from experimental groups (H&E staining ×400, scale bar = 50 µm). (**A**) Normal control group showing normal striated myocardial fibers with acidophilic cytoplasm and vesicular nuclei (arrows) and separated by few connective tissue containing fibroblasts with their flat nuclei (thick arrow). Most cardiac fibers display intercalated discs (arrowhead). Blood vessels are not congested (*). (**B**) SUN group displayed disordered myocardial structure with apparent inflammatory cellular infiltration (ovale). Myofibers are curly and have acidophilic cytoplasm with hyaline appearance (H). Some cardiac fibers are fragmented and dissolved (**D**). Most of the nuclei are dark and pyknotic (arrowhead). Wide spaces containing extravasated blood (S) and vacuoles (arrow) were seen between cardiac myofibrils. Blood

RETRACTED

vessels are congested (*). (**C**,**D**) represents SEC and BG groups, respectively, showed apparently better cardiac muscle structure with mild cellular inflammatory infiltrate (arrowhead) and congested blood vessels (*). Some cardiac muscle fibers have bright nuclei (arrow). Other muscles fibers are dissolved (**D**) and have dark shrunken nuclei (thick arrow) with hyaline outlook (H). Vacuoles (V) are present between the affected muscle fibers. SEC group exhibited the presence of intercalated discs (curved arrow). (**E**) SEC + BG group showed marked improvement in the cardiac muscle architecture with near to normal cardiac muscle structure. (**F**) Myofibril diameter (μm). NC: normal control; SUN: sunitinib; SEC: secukinumab; BG: black garlic. Bars with error bar represent mean ± SD. [a] $p < 0.001$ vs. NC, [b] $p < 0.001$ vs. SUN, [#] $p < 0.001$ vs. BG, [$] $p < 0.001$ vs. SEC.

SUN-ingested rats displayed various patchy areas of disturbed myocardial architecture with apparent vascular and interstitial congestion and inflammatory cellular infiltrates. This was identified in the innermost myocardial sub-endocardium of the apex of the left ventricle. Numerous cardiac muscle fibers were fragmented, swollen, and disturbed with vacuolations and extensive separations. Other fibers were strongly acidophilic and had hyaline outlines with loss of their typical transverse striations and intercalated discs. Most nuclei were dissolved and darkly stained (Figure 4B).

Secukinumab or black garlic-treated rats exhibited better myocardial structure, apart from mild inflammatory cellular infiltration and congestion. Many cardiac fibers were intact, while others had darkly stained nuclei. Only some myofibers had intensely acidophilic cytoplasm and hyaline outlook with some vacuoles and separation between cardiac muscle fibers (Figure 4C,D).

The combination of secukinumab with black garlic produced a drastic improvement in the cardiac muscle architecture with no inflammatory cellular infiltrate with minimally congested blood vessels. Most cardiac muscle fibers were striated with intercalated discs and bright vesicular nuclei. Few cardiac fibers had darkly stained nuclei. The maximum improvement was revealed in rats treated with both secukinumab and black garlic with a picture near to normal cardiac muscle fibers, striated cardiac fibers with bright centrally placed nuclei, and intact intercalated disc with no congested blood vessels or cellular infiltrates (Figure 4E).

The diameter of myofibers (in μm) was significantly increased in the sunitinib-treated hearts compared to control hearts. The use of secukinumab or black garlic decreased the myofibril diameter compared to the sunitinib-treated group. Amusingly, the combination of secukinumab with black garlic caused a strong reduction in the cardiac myofibril diameter compared to the sunitinib treated group and approaching the control group myofibril diameter (Figure 4F).

3.7.2. Van Gieson Stain

As illustrated in Figure 5A, the Van Gieson-stained heart section of the NC group revealed a normal histological structure without nearly any apparent myocardial fibrosis. On the contrary, the SUN group showed extensive collagen fibers in the interstitium between cardiomyocytes, indicating progression of cardiac fibrosis (Figure 5B). Less collagen fibers were observed in SEC and BG groups, indicating modest improvement in the fibrotic state induced by sunitinib (Figure 5C,D). Combining secukinumab with black garlic resulted in the least collagen deposition compared to the single treatments and showed the most protective effect against heart fibrosis (Figure 5E). In addition, our results showed a marked decrease in fibrosis % in all treated animals, with a specific promising effect in the SEC + BG group (Figure 5F).

RETRACTED

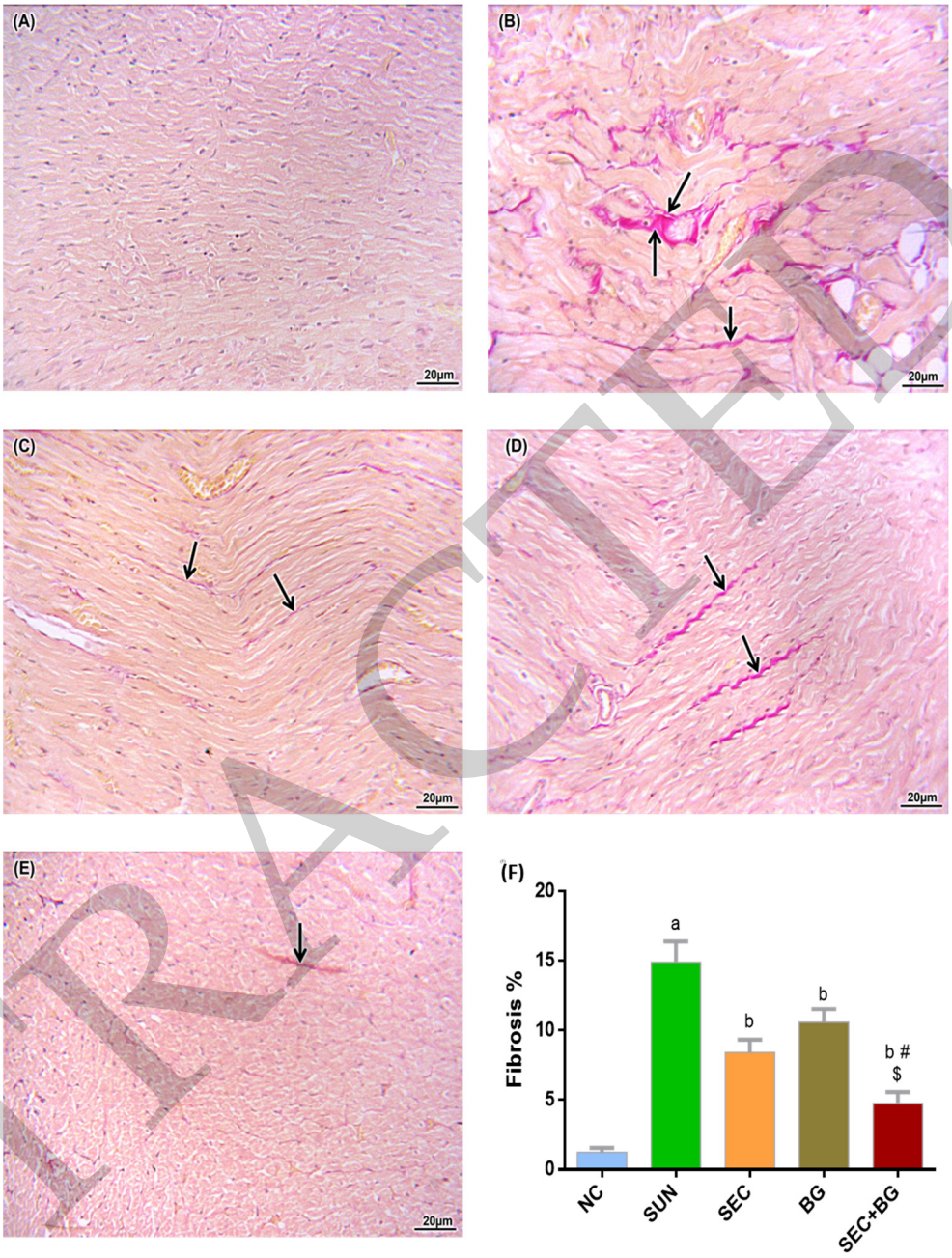


Figure 5. Representative photomicrographs of Van Gieson-stained sections of the heart (Van Gieson ×200, scale bar = 20 µm). (**A**) NC group showing a normal cardiac histological structure. (**B**) SUN group showing extensive collagen fibers indicated by the arrows. (**C**) SEC group showing few collagen fibers (arrows). (**D**) BG group showing moderate amount of collagen deposition (arrows). (**E**) SEC + BG group revealing remarkable reduction in collagen deposition with nearly normal structure (arrow). (**F**) Fibrosis%. NC: normal control; SUN: sunitinib; SEC: secukinumab; BG: black garlic; Red color indicates fibrosis. Bars with error bar represent mean ± SD. [a] $p < 0.001$ vs. NC, [b] $p < 0.001$ vs. SUN, [#] $p < 0.001$ vs. BG, [$] $p < 0.001$ vs. SEC.

4. Discussion

Despite the remarkable progress that has been achieved in the field of antineoplastic drug discovery, the off-target adverse effects continue to be massive obstacles. Amongst these adverse effects, cardiac fibrosis is one of the most important leading causes of death in oncology patients subsequent to tumor recurrence [35,36].

RETRACTED

The present study provided a novel mechanistic pathway that plays a part in sunitinib-induced cardiotoxicity, mainly interstitial myocardial fibrosis, which is efficiently ameliorated by the neutralization of IL-17 or supplementation with black garlic. Moreover, their co-administration exerted more antifibrotic effect than either individual drug. In this study, we verified our hypothesis and confirmed that IL-17 signals through the OPG/RANK/RANKL axis and involves in the interstitial myocardial fibrosis induced by sunitinib.

Cardiac fibrosis remains an unresolved problem that contributes to end-stage extra cellular matrix (ECM) remodeling and heart failure [37]. In the current study, rats that received SUN for four weeks demonstrated a marked decrease in body weight and a marked increase in heart weight and CI. In addition, hypertension and deteriorated cardiac function were observed as exhibited by marked rises in SBP, DBP, MBP, and HR besides a decline in LVEF% and FS% after administrating sunitinib in consistence with previous studies [2,38–41].

Moreover, a deleterious effect of SUN on the heart was emphasized by a drastic rise in serum CK-MB besides a significant inflammatory state, which concurred with the biochemical and histological features. The histological findings were manifested as fragmented cardiac muscle fibers with vacuolations and extensive separations along with excessive collagen depositions, in agreement with previous studies [5,27,42]. Hence, our results indicated that using SUN could be a promising model for studying the pathological mechanism of cardiac fibrosis and therapeutic interventions.

Greineder et al. demonstrated different signaling pathways through which SUN could mediate LV dysfunction and accordingly cardiotoxicity. He reported that SUN could impair the cardiac energy homeostasis mainly via mitochondrial dysfunction and inhibiting adenosine monophosphate-activated protein kinase. Additionally, platelet-derived growth factor receptors and vascular endothelial growth factor receptors, which are important in maintaining adult cardiac function, were found to be inhibited by sunitinib, resulting in LV dysfunction and heart failure [43].

It has been accounted that SUN stimulates NF-κB and sequentially mediates the release of pro-inflammatory cytokines [27,39,44,45]. Once NF-κB is activated, it is transported from the cytosol to the nucleus where it initiates the expression of many pro- and anti-inflammatory cytokines such as IL-17 [46,47]. In accordance, our data revealed an activated inflammatory state as evidenced by the raised levels of serum CRP, as well as cardiac NF-κB, IL-1β, IL-6, IL-17, and TNF-α after SUN administration.

It is well known that IL-17 receptors are expressed by any cell type and the circulating IL-17 regulates pleiotropic effects throughout the body and can act in cooperation with other mediators, such as IL-1β or TNF-α, to mediate additive or synergistic effects. Furthermore, IL-17 contributes to myocardial fibrosis through various mechanisms, including stimulation of cardiomyocyte death, enhancement of collagen production by cardiac fibroblasts, and activation of NF-κB [48,49]. It was found that IL-17 mediates its effect by interacting with transforming growth factor-β activated kinase 1 (TAK1) and IκB kinase complex (IKKβ) and promotes the formation of TAK1/IKK complex. This leads to upregulation of IKKβ/NF-κB, with consequent downstream activation of more IL-6 and TNF-α [50].

OPG is an extracellular matrix-associated protein and an important negative regulator of RANKL/RANK signaling pathway in bone matrix homeostasis [51]. Many studies indicated its involvement in several other physiological and pathological processes, including hypertension, ventricular remodeling, and heart failure [15]. A recent study illustrated that OPG can prompt cardiomyocytes hypertrophy through inhibiting autophagy, which is mediated by Focal Adhesion Kinase/(FAK/Beclin1) pathway [52]. In addition, high levels of OPG were found in fibrotic liver, heart, and vascular tissue that advocate a significant role for OPG in developing fibrosis [51,53–56]. Importantly, Liu et al. established that the OPG/RANK/RANKL system participated in the process of IL-17-associated myocardial remodeling and fibrosis [57].

In cardiac fibroblasts, IL-17A promotes inflammation and increases the expression of MMPs, TIMPs, and collagen, leading to fibroblast migration and myocardial remodeling, in

RETRACTED

which the excess interstitial collagen accumulation is considered a hallmark of myocardial fibrosis [58]. Collagen formation and disintegration are governed by the balanced activity of MMPs and their inhibitors, TIMPs. While MMP1 is responsible for degradation of collagen type I and III, in the main constituents of the heart's ECM, TIMP1 specifically binds to MMP1and regulates its action [59].

Given the fact that cardiac fibrosis is accompanied by increased MMP1 and TIMP1 levels, they can be employed as valuable fibrotic markers in both animals and patients with cardiovascular diseases [60]. In agreement, our results showed that SUN-administered rats exhibited upregulated MMP1 and TIMP1 expression in contrast to the downregulated MMP1/TIMP1 ratio.

Preceding studies confirmed the association of IL-17 with the OPG/RANK/RANKL system, in which IL-17 promotes RANK and RANKL expressions via NF-κB activity in different cell types and so disrupts the RANKL/OPG balance [61–63]. Additionally, increased RANKL expression markedly enhances MMP activity in human cardiac fibroblasts, with a particularly enhancing effect on MMP1, which suggests a potential mechanism by which increased RANKL expression contributes to LV remodeling and dysfunction [64,65].

Consistently with the aforementioned facts, the present study provides new evidence on the participation of the OPG/RANK/RANKL axis as one of the main mechanisms involved in sunitinib-induced interstitial MF.

Herein, neutralization of IL-17 by SEC effectively decreased heart weight and CI, in addition to increasing body weight almost to the normal values. In addition, SEC efficiently decreased CK-MB and restored normal BP readings besides improving LVEF% and FS% in the SEC-treated animals. The effects of IL-17 on arterial hypertension are not completely identified [66]. However, it has been shown that mice deficient in IL-17 were protected against aortic stiffening and the blockage of IL-17 effectively reduced arterial hypertension in rats [53,67]. Nguyen et al. demonstrated also that IL-17A induces phosphorylation of the inhibitory site on endothelial nitric oxide synthase, leading to decreased nitric oxide production via a Rho-kinase dependent pathway [68]. Another study reported that the levels of IL-17 were much lower in normotensive individuals than in those with hypertension [69], and targeting IL-17 might help to control blood pressure and conserve vascular function [70].

Concerning its effect on cardiac functions, IL-17 also proved to promote contractile dysfunction mainly through NF-κB-mediated disturbance of calcium handling and cardiac remodeling [71]. In our study, treatment with SEC successfully improved cardiac functions and lowered the cardiac levels of IL-1β, IL-6, IL-17, and TNF-α, in addition to considerable downregulation in the OPG/RANK/RANKL axis and normalization of the MMP1/TIMP ratio. Interestingly, all these effects were accompanied with restoring the normal architecture of cardiac tissues and a valuable decrease in collagen fibers content. This promising antifibrotic effect of secukinumab, in addition to its improved effects on cardiac functions, is owed mostly to its inhibition to IL-17 and accordingly inactivation of NF-κB and downregulation of the OPG/RANK/RANKL axis and improving the MMP1/TIMP1 ratio, as shown by our results.

Black garlic is a kind of deep-processed food made of fresh garlic under high temperatures and humidity [47]. Recent studies have reported many antioxidant and inflammatory effects in addition to other biological functions, such as anti-cancer, hepatoprotective, and cardioprotective effects. The health benefits of BG intake are mainly associated with the presence of bioactive substances such as phenol and organosulfur. These bioactive components of BG show a wide range of physiological functions in the human body, which may possibly have a therapeutic potential for treating a variety of diseases [19,72–75].

Here, BG-administrated rats showed valuable decreases in BP readings, improved LVEF% and heart function. This effect is mainly due to the presence of a high amount of SAC and flavonoids which act as effective antioxidants. These antioxidants can abolish the harmful effects of reactive oxygen species, especially their role in mediating cardiac

RETRACTED

hypertrophy, and thereby reducing the thickness of the heart wall, in agreement with preceding studies [75–79].

These valuable effects of BG supplementation were also associated with a marked decrease in collagen fibers deposition in the cardiac tissues besides significant decrease in cardiac IL-1β, IL-6, and TNF-α levels. All these findings are in agreement with Kim et al. who demonstrated marked reductions in IL-1β, IL-6, and TNF-α levels after using BG in a model of reflux esophagitis, which is mostly owing to inactivation of the NF-κB signaling pathway [80] by SAC [81]. Moreover, Anandasadagopan et al. reported that treatment with SAC could downregulate the expression of p65-NF-κB, TNF-α, and suppressed liver inflammation in a chromium-induced hepatotoxicity model [82]. Additionally, Kim et al. reported that BG was able to decrease the inflammatory response by modulating the transcriptional level of TNF-alpha mRNA and IL-6 [83]. In accordance with this, our data exhibited a significant decrease in cardiac NF-κB, in addition to the other inflammatory mediators after treatment with BG.

It was very interesting that our results showed noticeable downregulation of the OPG/RANK/RANKL axis and improvement in the MMP1/TIMP1 ratio after supplementation with BG, which was most likely due to the inhibition of cardiac NF-κB by SAC and consequently IL-17. Thus, this may explain the improving effect of SEC + BG co-administration in all biochemical parameters and histological findings over SEC or BG alone.

5. Conclusions

Conclusively, the present study shows a novel finding that administration of SUN upregulates the OPG/RANK/RANKL axis via activation of cardiac NF-κB and increases IL-17, which leads to a disruption in the MMP/TIMP ratio and eventually development of myocardial interstitial fibrosis. Neutralization of IL-17 by secukinumab effectively ameliorated MF induced by sunitinib through downregulating the OPG/RANK/RANKL axis mainly via inactivation of NF-κB, decreasing the IL-17 level, and improving the MMP1/TIMP1 ratio. Additionally, supplementing the experimental rats with black garlic was able to reverse sunitinib-induced cardiac fibrosis by the same mechanism but to a lesser extent than secukinumab. However, co-administration of secukinumab with black garlic showed additional valuable benefits against myocardial interstitial fibrosis than individual drugs. Further preclinical and clinical studies are warranted to confirm these results.

Supplementary Materials: The following supporting information can be downloaded at: https://www.mdpi.com/article/10.3390/life13020308/s1, Figure S1: Representative photomicrographs of H&E-stained cardiac sections (H&E staining ×400, scale bar = 20 μm); Table S1: Effect of treatment with sunitinib (25 mg/kg three times a week) orally for 4 weeks on serum CRP and CK-MB levels; Figure S2: Sequence and structural alignments human IL17 A, IL17 A mouse, and rat IL17 A; Table S2: BLAST analysis between human IL17 A and both IL17 A mouse and rat.

Author Contributions: Conceptualization, H.E.M. and M.E.A.; Data curation, O.I.F. and A.A.; Formal analysis, M.A.S., N.M.B. and Y.K.M.; Funding acquisition, O.I.F. and A.A.; Investigation, N.M.B. and Y.K.M.; Methodology, M.A.S., N.M.B., A.E.S. and Y.K.M.; Resources, N.M.B. and Y.K.M.; Supervision, H.E.M. and M.E.A.; Writing—original draft, N.M.B. and Y.K.M.; Writing—review & editing, H.E.M., M.E.A., N.M.B., O.I.F., A.A. and Y.K.M. All authors have read and agreed to the published version of the manuscript.

Funding: This research was funded by Researchers Supporting Project number (RSP2022R430), King Saud University, Riyadh, Saudi Arabia.

Institutional Review Board Statement: This study was conducted in accordance with NIH guidelines for animal research. Animal care and all experimental procedures were executed according to protocols approved by the institutional committee of laboratory animal care and use of Zagazig University (Protocol # ZU-IACUC/3/F/183/2021).

Informed Consent Statement: Not applicable.

RETRACTED

Data Availability Statement: The data presented in this study are available upon request from the corresponding author.

Acknowledgments: Researchers Supporting Project number (RSP2022R430), King Saud University, Riyadh, Saudi Arabia. The authors also acknowledge the support provided by the Faculty of Pharmacy, Zagazig University for the use of the animal unit facility.

Conflicts of Interest: The authors declare no conflict of interest.

References

1. Gorini, S.; De Angelis, A.; Berrino, L.; Malara, N.; Rosano, G.; Ferraro, E. Chemotherapeutic Drugs and Mitochondrial Dysfunction: Focus on Doxorubicin, Trastuzumab, and Sunitinib. *Oxid. Med. Cell. Longev.* **2018**, *2018*, 7582730. [CrossRef] [PubMed]
2. Yang, Y.; Bu, P. Progress on the cardiotoxicity of sunitinib: Prognostic significance, mechanism and protective therapies. *Chem. Biol. Interact.* **2016**, *257*, 125–131. [CrossRef] [PubMed]
3. Richards, C.J.; Je, Y.; Schutz, F.; Heng, D.; Dallabrida, S.; Moslehi, J.; Choueiri, T.K. Incidence and Risk of Congestive Heart Failure in Patients with Renal and Nonrenal Cell Carcinoma Treated with Sunitinib. *J. Clin. Oncol.* **2011**, *29*, 3450–3456. [CrossRef]
4. Formiga, M.N.; Fanelli, M.F. Aortic dissection during antiangiogenic therapy with sunitinib. *A case report. Sao Paulo Med. J.* **2015**, *133*, 275–277. [CrossRef] [PubMed]
5. Sourdon, J.; Facchin, C.; Certain, A.; Viel, T.; Robin, B.; Lager, F.; Marchiol, C.; Balvay, D.; Yoganathan, T.; Favier, J.; et al. Sunitinib-induced cardiac hypertrophy and the endothelin axis. *Theranostics* **2021**, *11*, 3830–3838. [CrossRef]
6. Kania, G.; Blyszczuk, P.; Eriksson, U. Mechanisms of cardiac fibrosis in inflammatory heart disease. *Trends Cardiovasc. Med.* **2009**, *19*, 247–252. [CrossRef]
7. Yoshida, A.; Kanamori, H.; Naruse, G.; Minatoguchi, S.; Iwasa, M.; Yamada, Y.; Mikami, A.; Kawasaki, M.; Nishigaki, K.; Minatoguchi, S. (Pro)renin Receptor Blockade Ameliorates Heart Failure Caused by Chronic Kidney Disease. *J. Card. Fail.* **2019**, *25*, 286–300. [CrossRef]
8. Lambert, J.M.; Lopez, E.F.; Lindsey, M.L. Macrophage roles following myocardial infarction. *Int. J. Cardiol.* **2008**, *130*, 147–158. [CrossRef]
9. Prabhu, S.D.; Frangogiannis, N.G. The Biological Basis for Cardiac Repair after Myocardial Infarction: From Inflammation to Fibrosis. *Circ. Res.* **2016**, *119*, 91–112. [CrossRef]
10. Anzai, T. Inflammatory Mechanisms of Cardiovascular Remodeling. *Circ. J.* **2018**, *82*, 629–635. [CrossRef]
11. Rochette, L.; Meloux, A.; Rigal, E.; Zeller, M.; Malka, G.; Cottin, Y.; Vergely, C. The Role of Osteoprotegerin in Vascular Calcification and Bone Metabolism: The Basis for Developing New Therapeutics. *Calcif. Tissue Int.* **2019**, *105*, 239–251. [CrossRef]
12. Lv, W.T.; Du, D.; Gao, R.; Yu, C.; Jia, Y.; Jia, Z.; Wang, C. Regulation of Hedgehog signaling Offers A Novel Perspective for Bone Homeostasis Disorder Treatment. *Int. J. Mol. Sci.* **2019**, *20*, 3981. [CrossRef]
13. Feng, W.; Li, W.; Liu, W.; Wang, F.; Li, Y.; Yan, W. IL-17 induces myocardial fibrosis and enhances RANKL/OPG and MMP/TIMP signaling in isoproterenol-induced heart failure. *Exp. Mol. Pathol.* **2009**, *87*, 212–218. [CrossRef]
14. Hao, Y.; Tsuruda, T.; Sekita-Hatakeyama, Y.; Kurogi, S.; Kubo, K.; Sakamoto, S.; Nakamura, M.; Udagawa, N.; Sekimoto, T.; Hatakeyama, K.; et al. Cardiac hypertrophy is exacerbated in aged mice lacking the osteoprotegerin gene. *Cardiovasc. Res.* **2016**, *110*, 62–72. [CrossRef] [PubMed]
15. Lu, J.; Liu, F.; Liu, D.; Du, H.; Hao, J.; Yang, X.; Cui, W. Amlodipine and atorvastatin improved hypertensive cardiac hypertrophy through regulation of receptor activator of nuclear factor kappa B ligand/receptor activator of nuclear factor kappa B/osteoprotegerin system in spontaneous hypertension rats. *Exp. Biol. Med.* **2016**, *241*, 1237–1249. [CrossRef]
16. Baeten, D.; Sieper, J.; Braun, J.; Baraliakos, X.; Dougados, M.; Emery, P.; Deodhar, A.; Porter, B.; Martin, R.; Andersson, M.; et al. Secukinumab, an Interleukin-17A Inhibitor, in Ankylosing Spondylitis. *N. Engl. J. Med.* **2015**, *373*, 2534–2548. [CrossRef]
17. Frieder, J.; Kivelevitch, D.; Menter, A. Secukinumab: A review of the anti-IL-17A biologic for the treatment of psoriasis. *Ther. Adv. Chronic Dis.* **2018**, *9*, 5–21. [CrossRef] [PubMed]
18. Karatas, A.; Celik, C.; Oz, B.; Akar, Z.; Etem, E.; Dagli, A.; Koca, S.S. Secukinumab and metformin ameliorate dermal fibrosis by decreasing tissue interleukin-17 levels in bleomycin-induced dermal fibrosis. *Int. J. Rheum. Dis.* **2021**, *24*, 795–802. [CrossRef] [PubMed]
19. Ahmed, T.; Wang, C.-K. Black Garlic and Its Bioactive Compounds on Human Health Diseases: A Review. *Molecules* **2021**, *26*, 5028. [CrossRef] [PubMed]
20. Allison, G.L.; Lowe, G.M.; Rahman, K. Aged Garlic Extract and Its Constituents Inhibit Platelet Aggregation through Multiple Mechanisms. *J. Nutr.* **2006**, *136*, 782S–788S. [CrossRef] [PubMed]
21. Colín-González, A.L.; Santana, R.; Silva-Islas, C.; Chánez-Cárdenas, M.; Santamaría, A.; Maldonado, P. The Antioxidant Mechanisms Underlying the Aged Garlic Extract- and S-Allylcysteine-Induced Protection. *Oxid. Med. Cell. Longev.* **2012**, *2012*, 907162. [CrossRef] [PubMed]
22. Moreira, A.S.P.; Nunes, F.; Domingues, M.; Coimbra, M. Coffee melanoidins: Structures, mechanisms of formation and potential health impacts. *Food Funct.* **2012**, *3*, 903–915. [CrossRef] [PubMed]
23. Colín-González, A.L.; Ali, S.; Túnez, I.; Santamaría, A. On the antioxidant, neuroprotective and anti-inflammatory properties of S-allyl cysteine: An update. *Neurochem. Int.* **2015**, *89*, 83–91. [CrossRef]

RETRACTED

24. Padmanabhan, M.; Prince, P.S. Preventive effect of S-allylcysteine on lipid peroxides and antioxidants in normal and isoproterenol-induced cardiotoxicity in rats: A histopathological study. *Toxicology* **2006**, *224*, 128–137. [CrossRef] [PubMed]
25. Czompa, A.; Szoke, K.; Prokisch, J.; Gyongyosi, A.; Bak, I.; Balla, G.; Tosaki, A.; Lekli, I. Aged (Black) versus Raw Garlic against Ischemia/Reperfusion-Induced Cardiac Complications. *Int. J. Mol. Sci.* **2018**, *19*, 1017. [CrossRef]
26. Oztanir, M.N.; Dogan, M.; Turkmen, N.; Taslidere, A.; Sahin, Y.; Ciftci, O. Secukinumab Ameliorates Oxidative Damage Induced by Cerebral Ischemia-Reperfusion in Rats. *Turk. Neurosurg.* **2022**, *32*, 732–739. [CrossRef] [PubMed]
27. Imam, F.; Al-Harbi, N.; Khan, M.; Qamar, W.; Alharbi, M.; Alshamrani, A.; Alhamami, H.; Alsaleh, N.; Alharbi, K. Protective Effect of RIVA Against Sunitinib-Induced Cardiotoxicity by Inhibiting Oxidative Stress-Mediated Inflammation: Probable Role of TGF-β and Smad Signaling. *Cardiovasc. Toxicol.* **2020**, *20*, 281–290. [CrossRef] [PubMed]
28. Polegato, B.F.; Minicucci, M.; Azevedo, P.; Carvalho, R.; Chiuso-Minicucci, F.; Pereira, E.; Paiva, S.; Zornoff, L.; Okoshi, M.; Matsubara, B.; et al. Acute doxorubicin-induced cardiotoxicity is associated with matrix metalloproteinase-2 alterations in rats. *Cell. Physiol. Biochem.* **2015**, *35*, 1924–1933. [CrossRef] [PubMed]
29. Lang, R.M.; Badano, L.; Victor, M.; Afilalo, J.; Armstrong, A.; Ernande, L.; Flachskampf, F.; Foster, E.; Goldstein, S.; Kuznetsova, T.; et al. Recommendations for cardiac chamber quantification by echocardiography in adults: An update from the American Society of Echocardiography and the European Association of Cardiovascular Imaging. *J. Am. Soc. Echocardiogr.* **2015**, *28*, 1. [CrossRef]
30. Parasuraman, S.; Raveendran, R. Measurement of invasive blood pressure in rats. *J. Pharmacol. Pharmacother.* **2012**, *3*, 172–177.
31. Wu, M.; Guo, Y.; Wu, Y.; Xu, K.; Lin, L. Protective Effects of Sacubitril/Valsartan on Cardiac Fibrosis and Function in Rats with Experimental Myocardial Infarction Involves Inhibition of Collagen Synthesis by Myocardial Fibroblasts through Downregulating TGF-β1/Smads Pathway. *Front. Pharmacol.* **2021**, *12*, 696472. [CrossRef] [PubMed]
32. Lanoix, D.; Ouellette, R.; Vaillancourt, C. Expression of melatoninergic receptors in human placental choriocarcinoma cell lines. *Hum. Reprod.* **2006**, *21*, 1981–1989. [CrossRef] [PubMed]
33. Bradford, M.M. A rapid and sensitive method for the quantitation of microgram quantities of protein utilizing the principle of protein-dye binding. *Anal. Biochem.* **1976**, *72*, 248–254. [CrossRef] [PubMed]
34. Jain, P.; Arava, S.; Seth, S.; Lalwani, S.; Ray, R. Histological and morphometric analysis of dilated cardiomyopathy with special reference to collagen IV expression. *Indian J. Pathol. Microbiol.* **2017**, *60*, 481–486.
35. Godishala, A.; Yang, S.; Asnani, A. Cardioprotection in the Modern Era of Cancer Chemotherapy. *Cardiol. Rev.* **2018**, *26*, 113–121. [CrossRef]
36. Jain, D.; Aronow, W. Cardiotoxicity of cancer chemotherapy in clinical practice. *Hosp. Pract.* **2019**, *47*, 6–15. [CrossRef] [PubMed]
37. Liu, M.; de Juan Abad, B.L.; Cheng, K. Cardiac fibrosis: Myofibroblast-mediated pathological regulation and drug delivery strategies. *Adv. Drug Deliv. Rev.* **2021**, *173*, 504–519. [CrossRef] [PubMed]
38. Bæk Møller, N.; Budolfsen, C.; Grimm, D.; Krüger, M.; Infanger, M.; Wehland, M.; Magnusson, N.E. Drug-induced hypertension caused by multikinase inhibitors (sorafenib, sunitinib, lenvatinib and axitinib) in renal cell carcinoma treatment. *Int. J. Mol. Sci.* **2019**, *20*, 4712. [CrossRef]
39. Blanca, A.J.; Ruiz-Armenta, M.; Zambrano, S.; Miguel-Carrasco, J.; Arias, J.; Arévalo, M.; Mate, A.; Aramburu, O.; Vázquez, C.M. Inflammatory and fibrotic processes are involved in the cardiotoxic effect of sunitinib: Protective role of L-carnitine. *Toxicol. Lett.* **2016**, *241*, 9–18. [CrossRef]
40. Ren, C.; Sun, K.; Zhang, Y.; Hu, Y.; Hu, B.; Zhao, J.; He, Z.; Ding, R.; Wang, W.; Liang, C. Sodium–glucose cotransporter-2 inhibitor empagliflozin ameliorates sunitinib-induced cardiac dysfunction via regulation of AMPK–mTOR signaling pathway–mediated autophagy. *Front. Pharmacol.* **2021**, *12*, 664181. [CrossRef]
41. Yang, Y.; Li, N.; Chen, T.; Zhang, C.; Liu, L.; Qi, Y.; Bu, P. Trimetazidine ameliorates sunitinib-induced cardiotoxicity in mice via the AMPK/mTOR/autophagy pathway. *Pharm. Biol.* **2019**, *57*, 625–631. [CrossRef] [PubMed]
42. Sayed-Ahmed, M.M.; Alrufaiq, B.; Alrikabi, A.; Abdullah, M.; Hafez, M.; Al-Shabanah, O. Carnitine Supplementation Attenuates Sunitinib-Induced Inhibition of AMP-Activated Protein Kinase Downstream Signals in Cardiac Tissues. *Cardiovasc. Toxicol.* **2019**, *19*, 344–356. [CrossRef] [PubMed]
43. Greineder, C.F.; Kohnstamm, S.; Ky, B. Heart failure associated with sunitinib: Lessons learned from animal models. *Curr. Hypertens. Rep.* **2011**, *13*, 436–441. [CrossRef] [PubMed]
44. Aldemir, M.; Simsek, M.; Kara, A.; Ozcicek, F.; Mammadov, R.; Yazıcı, G.; Sunar, M.; Coskun, R.; Gulaboglu, M.; Suleyman, H. The effect of adenosine triphosphate on sunitinib-induced cardiac injury in rats. *Hum. Exp. Toxicol.* **2020**, *39*, 1046–1053. [CrossRef]
45. Liu, T.; Zhang, L.; Joo, D.; Sun, S.-C. NF-κB signaling in inflammation. *Signal Transduct. Target. Ther.* **2017**, *2*, 17023. [CrossRef]
46. Molinero, L.L.; Cubre, A.; Mora-Solano, C.; Wang, Y.; Alegre, M.-L. T cell receptor/CARMA1/NF-κB signaling controls T-helper (Th) 17 differentiation. *Proc. Natl. Acad. Sci. USA* **2012**, *109*, 18529–18534. [CrossRef] [PubMed]
47. Sode, J.; Bank, S.; Vogel, U.; Andersen, P.; Sørensen, S.; Bojesen, A.; Andersen, M.; Brandslund, I.; Dessau, R.; Hoffmann, H.; et al. Genetically determined high activities of the TNF-alpha, IL23/IL17, and NFkB pathways were associated with increased risk of ankylosing spondylitis. *BMC Med. Genet.* **2018**, *19*, 165. [CrossRef]
48. Murugaiyan, G.; Saha, B. Protumor vs Antitumor Functions of IL-17. *J. Immunol.* **2009**, *183*, 4169–4175. [CrossRef]
49. Robert, M.; Miossec, P. Effects of Interleukin 17 on the cardiovascular system. *Autoimmun. Rev.* **2017**, *16*, 984–991. [CrossRef]
50. Jiang, Y.; Tian, M.; Lin, W.; Wang, X.; Wang, X. Protein kinase serine/threonine kinase 24 positively regulates interleukin 17-induced inflammation by promoting IKK complex activation. *Front. Immunol.* **2018**, *9*, 921. [CrossRef]

RETRACTED

51. Habibie, H.; Adhyatmika, A.; Schaafsma, D.; Melgert, B. The role of osteoprotegerin (OPG) in fibrosis: Its potential as a biomarker and/or biological target for the treatment of fibrotic diseases. *Pharmacol. Ther.* **2021**, *228*, 107941. [CrossRef] [PubMed]
52. Zheng, D.; Zhang, M.; Liu, T.; Zhou, T.; Shen, A. Osteoprotegerin prompts cardiomyocyte hypertrophy via autophagy inhibition mediated by FAK/BECLIN1 pathway. *Life Sci.* **2021**, *264*, 118550. [CrossRef] [PubMed]
53. Wu, J.; Thabet, S.; Kirabo, A.; Trott, D.; Saleh, M.; Xiao, L.; Madhur, M.; Chen, W.; Harrison, D. Inflammation and mechanical stretch promote aortic stiffening in hypertension through activation of p38 mitogen-activated protein kinase. *Circ. Res.* **2014**, *114*, 616–625. [CrossRef]
54. Cortez, D.M.; Feldman, M.D.; Mummidi, S.; Valente, A.; Steffensen, B.; Vincenti, M.; Barnes, J.; Chandrasekar, B. IL-17 stimulates MMP-1 expression in primary human cardiac fibroblasts via p38 MAPK-and ERK1/2-dependent C/EBP-β, NF-κB, and AP-1 activation. *Am. J. Physiol. Heart Circ. Physiol.* **2007**, *293*, H3356–H3365. [CrossRef]
55. Toffoli, B.; Pickering, R.J.; Tsorotes, D.; Wang, B.; Bernardi, S.; Kantharidis, P.; Fabris, B.; Zauli, G.; Secchiero, P.; Thomas, M. Osteoprotegerin promotes vascular fibrosis via a TGF-β1 autocrine loop. *Atherosclerosis* **2011**, *218*, 61–68. [CrossRef]
56. Boorsma, C.E.; Draijer, C.; Cool, R.; Brandsma, C.; Nossent, G.; Brass, D.; Timens, W.; Melgert, B. A29 New Kids on the Fibrotic Block: Lung Fibrosis and Fibroblast Biology: A Possible Role for the Rank/rankl/opg Axis in Pulmonary Fibrosis. *Am. J. Respir. Crit. Care Med.* **2014**, *189*, 1.
57. Liu, W.; Feng, W.; Wang, F.; Li, W.; Gao, C.; Zhou, B.; Ma, M. Osteoprotegerin/RANK/RANKL axis in cardiac remodeling due to immuno-inflammatory myocardial disease. *Exp. Mol. Pathol.* **2008**, *84*, 213–217. [CrossRef] [PubMed]
58. Kong, P.; Christia, P.; Frangogiannis, N.G. The pathogenesis of cardiac fibrosis. *Cell. Mol. Life Sci.* **2014**, *71*, 549–574. [CrossRef] [PubMed]
59. Li, Y.Y.; McTiernan, C.F.; Feldman, A.M. Interplay of matrix metalloproteinases, tissue inhibitors of metalloproteinases and their regulators in cardiac matrix remodeling. *Cardiovasc. Res.* **2000**, *46*, 214–224. [CrossRef]
60. Takawale, A.; Zhang, P.; Patel, V.; Wang, X.; Oudit, G.; Kassiri, Z. Tissue inhibitor of matrix metalloproteinase-1 promotes myocardial fibrosis by mediating CD63–integrin β1 interaction. *Hypertension* **2017**, *69*, 1092–1103. [CrossRef]
61. Chen, X.-W.; Zhou, S.-F. Inflammation, cytokines, the IL-17/IL-6/STAT3/NF-κB axis, and tumorigenesis. *Drug Des. Dev. Ther.* **2015**, *9*, 2941.
62. Me, R.; Gao, N.; Dai, C.; Fu-Shin, X. IL-17 Promotes pseudomonas aeruginosa keratitis in C57BL/6 mouse corneas. *J. Immunol.* **2020**, *204*, 169–179. [CrossRef] [PubMed]
63. Bi, C.S.; Sun, L.; Qu, H.; Chen, F.; Tian, B.; Chen, F. The relationship between T-helper cell polarization and the RANKL/OPG ratio in gingival tissues from chronic periodontitis patients. *Clin. Exp. Dent. Res.* **2019**, *5*, 377–388. [CrossRef] [PubMed]
64. Ueland, T.; Yndestad, A.; Øie, E.; Florholmen, G.; Halvorsen, B.; Frøland, S.; Simonsen, S.; Christensen, G.; Gullestad, L.; Aukrust, P. Dysregulated osteoprotegerin/RANK ligand/RANK axis in clinical and experimental heart failure. *Circulation* **2005**, *111*, 2461–2468. [CrossRef]
65. Dutka, M.; Bobiński, R.; Wojakowski, W.; Francuz, T.; Pająk, C.; Zimmer, K. Osteoprotegerin and RANKL-RANK-OPG-TRAIL signalling axis in heart failure and other cardiovascular diseases. *Heart Fail. Rev.* **2021**, *27*, 1395–1411. [CrossRef] [PubMed]
66. Beringer, A.; Miossec, P. Systemic effects of IL-17 in inflammatory arthritis. *Nat. Rev. Rheumatol.* **2019**, *15*, 491–501. [CrossRef] [PubMed]
67. Amador, C.A.; Barrientos, V.; Peña, J.; Herrada, A.; González, M.; Valdés, S.; Carrasco, L.; Alzamora, R.; Figueroa, F.; Kalergis, A. Spironolactone decreases DOCA–salt–induced organ damage by blocking the activation of T helper 17 and the downregulation of regulatory T lymphocytes. *Hypertension* **2014**, *63*, 797–803. [CrossRef]
68. Nguyen, H.; Chiasson, V.; Chatterjee, P.; Kopriva, S.; Young, K.; Mitchell, B. Interleukin-17 causes Rho-kinase-mediated endothelial dysfunction and hypertension. *Cardiovasc. Res.* **2013**, *97*, 696–704. [CrossRef]
69. Madhur, M.S.; Lob, H.; McCann, L.; Iwakura, Y.; Blinder, Y.; Guzik, T.; Harrison, D. Interleukin 17 promotes angiotensin II–induced hypertension and vascular dysfunction. *Hypertension* **2010**, *55*, 500–507. [CrossRef]
70. de Morales, J.M.G.R.; Puig, L.; Daudén, E.; Cañete, J.; Pablos, J.; Martín, A.; Juanatey, C.; Adán, A.; Montalbán, X.; Borruel, N. Critical role of interleukin (IL)-17 in inflammatory and immune disorders: An updated review of the evidence focusing in controversies. *Autoimmun. Rev.* **2020**, *19*, 102429. [CrossRef]
71. Xue, G.-l.; Li, D.-s.; Wang, Z.-y.; Liu, Y.; Yang, J.-m.; Li, C.-z.; Li, X.-d.; Ma, J.-d.; Zhang, M.-m.; Lu, Y.-j. Interleukin-17 upregulation participates in the pathogenesis of heart failure in mice via NF-κB-dependent suppression of SERCA2a and Cav1. 2 expression. *Acta Pharmacol. Sin.* **2021**, *42*, 1780–1789. [CrossRef]
72. Tsai, J.-C.; Chen, Y.-A.; Wu, J.-T.; Cheng, K.-C.; Lai, P.-S.; Liu, K.-F.; Lin, Y.-K.; Huang, Y.-T.; Hsieh, C.-W. Extracts from Fermented Black Garlic Exhibit a Hepatoprotective Effect on Acute Hepatic Injury. *Molecules* **2019**, *24*, 1112. [CrossRef] [PubMed]
73. Dong, M.; Yang, G.; Liu, H.; Liu, X.; Lin, S.; Sun, D.; Wang, Y. Aged black garlic extract inhibits HT29 colon cancer cell growth via the PI3K/Akt signaling pathway. *Biomed. Rep.* **2014**, *2*, 250–254. [CrossRef]
74. Zhang, X.; Shi, Y.; Wang, L.; Li, X.; Zhang, S.; Wang, X.; Jin, M.; Hsiao, C.-D.; Lin, H.; Han, L.; et al. Metabolomics for Biomarker Discovery in Fermented Black Garlic and Potential Bioprotective Responses against Cardiovascular Diseases. *J. Agric. Food Chem.* **2019**, *67*, 12191–12198. [CrossRef]
75. Liu, J.; Zhang, G.; Cong, X.; Wen, C. Black Garlic Improves Heart Function in Patients with Coronary Heart Disease by Improving Circulating Antioxidant Levels. *Front. Physiol.* **2018**, *9*, 1435. [CrossRef] [PubMed]

RETRACTED

76. Ahmed, R.A. Hepatoprotective and antiapoptotic role of aged black garlic against hepatotoxicity induced by cyclophosphamide. *J. Basic Appl. Zool.* **2018**, *79*, 1–8. [CrossRef]
77. Setiawan, A.A.; Purnomo, F.; Karlowee, V.; Wijayahadi, N. The Effect of Black Garlic (*Allium sativum* Linn) on Cardiac and Aortic Histopathology in Experimental Studies in Obesity Rats. *J. Biomed. Transl. Res.* **2021**, *7*, 62–68. [CrossRef]
78. Ha, A.W.; Kim, W.K. Antioxidant mechanism of black garlic extract involving nuclear factor erythroid 2-like factor 2 pathway. *Nutr. Res. Pract.* **2017**, *11*, 206–213. [CrossRef]
79. Wang, K.; Dong, Y.; Liu, J.; Qian, L.; Wang, T.; Gao, X.; Wang, K.; Zhou, L. Effects of REDOX in regulating and treatment of metabolic and inflammatory cardiovascular diseases. *Oxid. Med. Cell. Longev.* **2020**, *2020*, 5860356. [CrossRef]
80. Kim, K.J.; Kim, S.; Shin, M.-R.; Kim, Y.; Park, H.-J.; Roh, S.-S. Protective effect of S-allyl cysteine-enriched black garlic on reflux esophagitis in rats via NF-κB signaling pathway. *J. Funct. Foods* **2019**, *58*, 199–206. [CrossRef]
81. Yudhistira, B.; Punthi, F.; Lin, J.; Sulaimana, A.; Chang, C.; Hsieh, C. S-Allyl cysteine in garlic (*Allium sativum*): Formation, biofunction, and resistance to food processing for value-added product development. *Compr. Rev. Food Sci. Food Saf.* **2022**, *21*, 2665–2687. [CrossRef] [PubMed]
82. Anandasadagopan, S.; Sundaramoorthy, C.; Pandurangan, A.; Nagarajan, V.; Srinivasan, K.; Ganapasam, S. S-Allyl cysteine alleviates inflammation by modulating the expression of NF-κB during chromium (VI)-induced hepatotoxicity in rats. *Hum. Exp. Toxicol.* **2017**, *36*, 1186–1200. [CrossRef] [PubMed]
83. Kim, M.J.; Yoo, Y.; Kim, H.; Shin, S.; Sohn, E.; Min, A.; Sung, N.; Kim, M. Aged black garlic exerts anti-inflammatory effects by decreasing no and proinflammatory cytokine production with less cytoxicity in LPS-stimulated raw 264.7 macrophages and LPS-induced septicemia mice. *J. Med. Food* **2014**, *17*, 1057–1063. [CrossRef] [PubMed]

Disclaimer/Publisher's Note: The statements, opinions and data contained in all publications are solely those of the individual author(s) and contributor(s) and not of MDPI and/or the editor(s). MDPI and/or the editor(s) disclaim responsibility for any injury to people or property resulting from any ideas, methods, instructions or products referred to in the content.

RETRACTED